


Quenching chaos in a power system using fixed-time fractional-order sliding mode controller

Abdul-Basset A. Al-Hussein* 

University of Basrah, College of Engineering, Electrical Engineering Department, Basrah, Iraq,
abdulbasset.jasim@uobasrah.edu.iq

Fadhil Rahma Tahir 

University of Basrah, College of Engineering, Electrical Engineering Department, Basrah, Iraq,
fadhil.rahma@uobasrah.edu.iq

Submitted: 10.02.2023

Accepted: 18.07.2023

Published: 30.09.2023



* Corresponding Author

Abstract: The aim of this paper is to study the unwanted chaotic oscillation that can severely affect the reliable and safe operation of electrical power systems. The dynamical behavior of a benchmark three-bus nonlinear electrical power system model is explored using modern nonlinear analysis methods, where the Lyapunov exponents spectrum, bifurcation diagram, power spectral density and bicoherence are used to investigate the chaotic oscillation in the power system. The analysis shows the existence of critical parameter values that may drive the power system to an unstable region and can expose the system to bus voltage collapse and angle divergence or blackout. To eliminate the chaotic oscillation, a fractional-order fixed time sliding mode controller has been used to control the power system in a finite time that can be predetermined by the designer. The Lyapunov theorem has been used to prove the stability of the controlled power system. The results confirm the superiority, robustness, and effectiveness of the suggested control algorithm.

Keywords: chaos, power stability, control, fixed-time stability, fractional order, sliding mode.

Cite this paper as: Al-Hussein, A.A., & Rahma Tahir, F., Quenching chaos in a power system using fixed-time fractional-order sliding mode controller. *Journal of Energy Systems* 2023; 7(3): 244-256, DOI: 10.30521/jes.1246901

1. INTRODUCTION

Electrical power systems are growing day by day to large-scale complex grids with many devices interconnected, such as buses, generators, transformers, and different types of linear and nonlinear loads. Due to the large expansion of energy demand, most of the power networks today work under stressed conditions, and closer to their limits of stability, and are threatened by the possibility of voltage and angle instability. Due in part to this operating environment, issues with the dynamic stability assessment of power systems are becoming more and more significant. Recent works show that electrical nonlinear power systems can undergo unavoidable chaotic behavior under certain circumstances and drive the power grid to voltage collapse and blackout [1,2].

From the early works [3,4,5,6], the authors investigated basic chaotic power systems with two connected buses using numerical analysis approaches. The scholars in Ref. [7] revealed the behavior of a three-node power system's bifurcation process and simplified the analysis by approximating the soft windup limiter with a smooth function. In a three-bus power system, researchers in Ref. [8] investigated the relationship between distinct instability modes and chaos occurrences, as well as the different routes to chaos. A power system of single-machine infinite-bus SMIB topology with a hard limit in the feedback loop of the excitation system has been presented in [9]. Therefore, controlling the chaotic disorder in electrical power networks has been an important research topic. Many nonlinear control methods have been designed for the suppression and quenching of chaotic oscillations in power systems. In Ref. [10], the authors used a linearized state feedback control method to eliminate chaotic dynamical behavior in a power system. The scholars in Ref. [11] suggested adaptive control methods for suppression of chaotic oscillations in power systems. The authors of Refs. [12,13] applied synergetic control theory to stabilize the dynamic of power systems to the equilibrium point, employing the analytical design of aggregated regulators (ADAR) method.

The application of fractional-calculus techniques in control permits a greater degree of freedom and offers promising strategies to design fractional-order controllers and provide better control performance comparable to integer-order control algorithms. In literature, there are many designed fractional-order controllers for instance the fractional-order optimal controller [14], fractional-order Takagi–Sugeno fuzzy controller based on interval theory [15], robust non-singular terminal sliding mode controller using fractional-order calculus proposed in Ref. [16]. A novel fractional-order with incommensurate order and linear augmentation control method is suggested in Ref. [17] to remove the coexistence of multiple attractors and chaos in the power system. All the aforementioned control techniques cannot ensure in advance a preallocated fixed convergence time to a stable equilibrium. Generally, the power system can only admit oscillation if it is damped within a short bounded time. Polyakov [18] first introduced the concept of fixed-time control in 2012. Fixed-time stability theory is an extended version of finite-time stability [19]. This method can maintain stronger robustness compared with the other control approaches and ensure a specified upper limit of convergence time [20].

Motivated by the above literature survey and discussion, this paper aims to provide new insight into the complex dynamic behaviours of a benchmark three-bus power system model. The main advantages and contributions of this work are listed as follows: 1) Analysis of the chaotic behaviors and period doubling is reported by varying the parameter values of the electrical power system consisting of three buses. 2) Use modern nonlinear analysis tools of bifurcation plots, Lyapunov exponents spectrum, power spectral density (PSD) and bicoherence measure to investigate the system dynamics. 3) Suggests a fractional-order fixed-time sliding mode control algorithm that effectively can reduce the convergence time, eliminate undesirable chaotic oscillation in the electrical system, and prevent bus voltage collapse. 4) The suggested controller's key advantages are that it can ensure the stability of the system in a limited time regardless of the system states initially and that the settling time to equilibrium is accurately

estimated in advance. 5) Lyapunov stability theory is employed to prove the finite-time convergence of the system state trajectories to the equilibrium condition.

The hierarchy of the paper is as follows: Sec. 2 introduces the mathematical representation of the chaotic power system. In Sec. 3, the dynamics of the system are investigated. The chaotic oscillations are considered with the parametrical variations. Then, Sec. 4 gives some definitions and lemmas and the derivation of the fixed-time fractional-order sliding mode control method. In Sec. 5, for validating the theoretical analysis, two simulation scenarios have been presented to demonstrate the controller robustness and effectiveness. In Sec. 6, we end with a conclusions sections where remarks are underlined.

2. MATHEMATICAL MODEL

The schematic diagram of the considered system as an electric connection is depicted in Fig. 1. The system is a reference benchmark scheme provided in Refs. [3,21], for investigating the stability of bus voltage and angle dynamics.

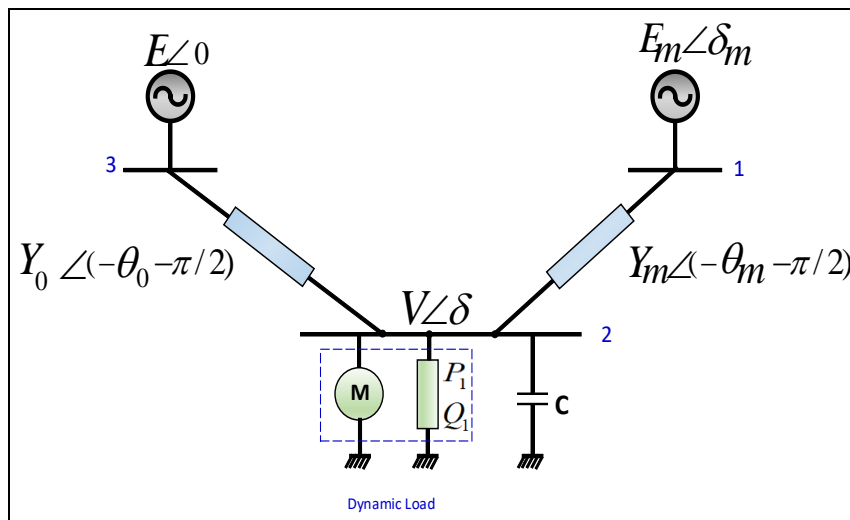


Figure 1. The scheme of the considered power system (1).

The proposed system includes three buses, bus numbered “1” is used to connect the generator and bus “2” is used to connect the load while bus “3” represents the infinite bus. The load bus is connected to an induction motor parallel to a constant $P-Q$ load. The dynamics of the power system can be represented in a four-dimensional mathematical model as follows:

$$\left\{ \begin{array}{l} \dot{\delta}_m = \omega = f_1, \\ M\dot{\omega} = -d_m\omega + P_m + E_m Y_m V \sin(\delta - \delta_m - \theta_m) \\ \quad + E_m^2 Y_m \sin \theta_m = M f_2, \\ K_{qw} \dot{\delta} = -K_{qv2} V^2 - K_{qv} V + E'_0 Y'_0 V \cos(\delta + \theta'_0) \\ \quad + E_m Y_m V \cos(\delta - \delta_m + \theta_m) - (Y'_0 \cos \theta'_0 \\ \quad + Y_m \cos \theta_m) V^2 - (Q_0 + Q_1) = K_{qw} f_3 \\ TK_{qw} K_{pv} \dot{V} = K_{pw} K_{qv2} V^2 + (K_{pw} K_{qv} - K_{qw} K_{pv}) V \\ \quad + \sqrt{K_{qw}^2 + K_{pw}^2} (-E'_0 Y'_0 V \cos(\delta + \theta'_0 - \psi) \\ \quad - E_m Y_m V \cos(\delta - \delta_m + \theta_m - \psi) + (Y'_0 \\ \quad \cos(\theta'_0 - \psi) + Y_m \cos(\theta_m - \psi)) V^2 - K_{qw} \\ \quad (P_0 + P_1) + K_{pw} (Q_0 + Q_1) = TK_{qw} K_{pv} f_4 \end{array} \right. , \quad (1)$$

where δ_m refers to the angle of the generator, the deviation in the operating frequency presented by ω , M parameter defines the synchronous generator inertia, d_m exemplifies the damping coefficient and P_m is the generator input power from the prime mover, θ_m and Y_m , respectively, are the impedance angle and the admittance of the transmission line, E_m represents the voltage magnitude value of the generator, V and δ , respectively, indicate the voltage magnitude of the load and the phase angle, $\psi = \tan^{-1} \left(\frac{K_{qw}}{K_{pw}} \right)$; Q_1 and P_1 are, respectively the constant reactive power and the real power of the connected

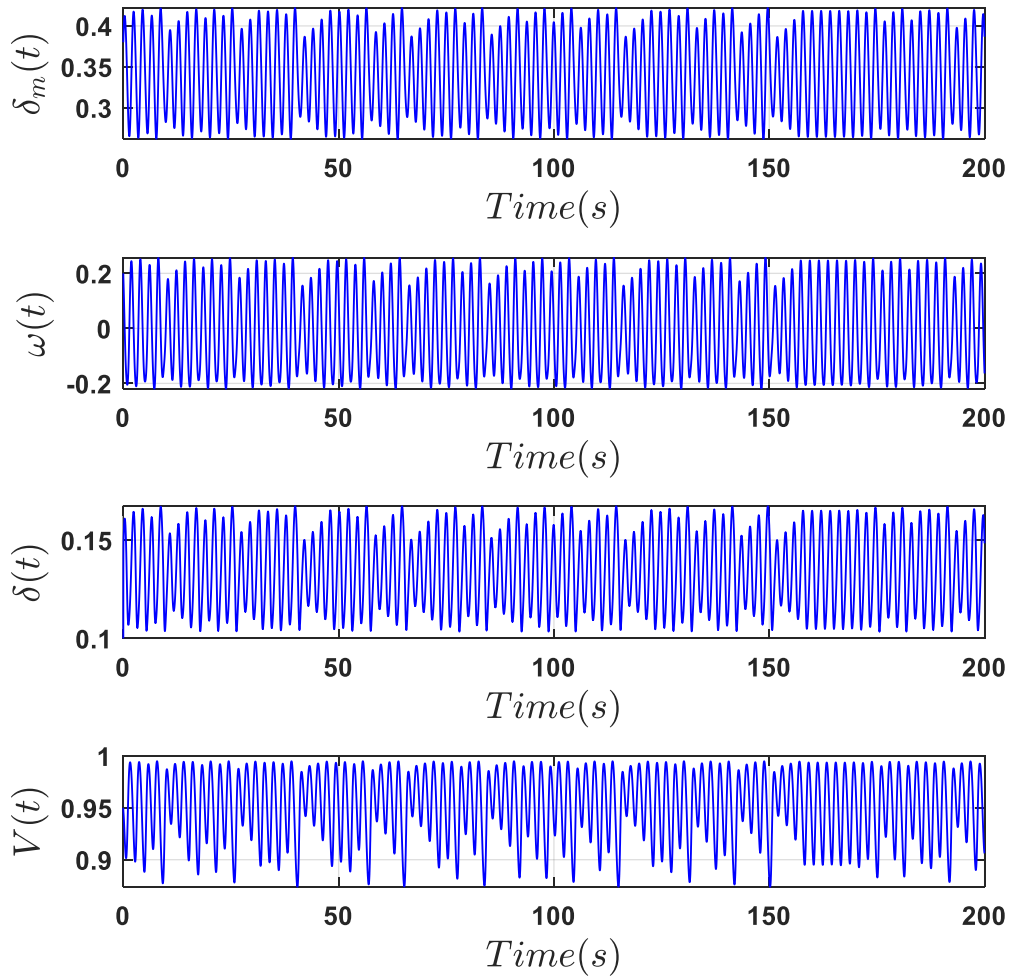


Figure 2. Waveforms and functions for the chaotic power system from Eq. (1).

load. On the other hand, the induction motor reactive power and real power are, respectively, denoted as Q_0 and P_0 . The motor parameters are denoted K_{pw} , K_{pv} , K_{qw} , K_{qv} , and K_{qv2} . Finally, Thevenin equivalent parameters are denoted as Y'_0 , θ'_0 , and E'_0 .

3. DYNAMICAL ANALYSIS

To study the dynamical characteristics and nature of the considered electrical system, the parameter Q_1 of the constant load, will be employed as a bifurcation coefficient. The electrical and mechanical parameters values are as follows [22]: $E_m = 1.0$, $Y_m = 5.0$, $\theta_m = -5.0$, $E'_0 = 2.5$, $Y'_0 = 8$, $\theta'_0 = -12$, $d_m = 0.05$, $M=0.3$, $K_{pw} = 0.4$, $K_{qv2} = 2.1$, $K_{qw} = -0.03$, $K_{qv} = -2.8$, $K_{pv} = 0.3$, $P_0 = 0.6$, $T = 8.5$, $Q_0 = 1.3$, $P_1 = 0$, $P_m = 1$. These values are considered in per unit bases other than the angles values θ_m and θ'_m given in rad. The initial condition is set as $(\delta_m(0), \omega(0), \delta(0), V(0)) = (0.38, 0.2, 0.1, 0.95)$.

The time responses of the power model and different projections of the electrical power system chaotic attractor at $Q_1 = 11.377$ are depicted, respectively, in Figs. 2 and 3. These diagrams emphasize how aperiodic the system is, with an irregular oscillation and strange attractors topology. By varying the bifurcation parameter Q_1 within $[11.37659, 11.3907]$ range, and recording the local maxima of the power system (1) state ω , the bifurcation diagram plotted as in given in Fig. 4. The bifurcation diagram plot shows that when $Q_1 \in [11.37659, 11.3818]$ the power system has a chaotic nature and with period-doubling root to chaos in the reverse direction is followed.

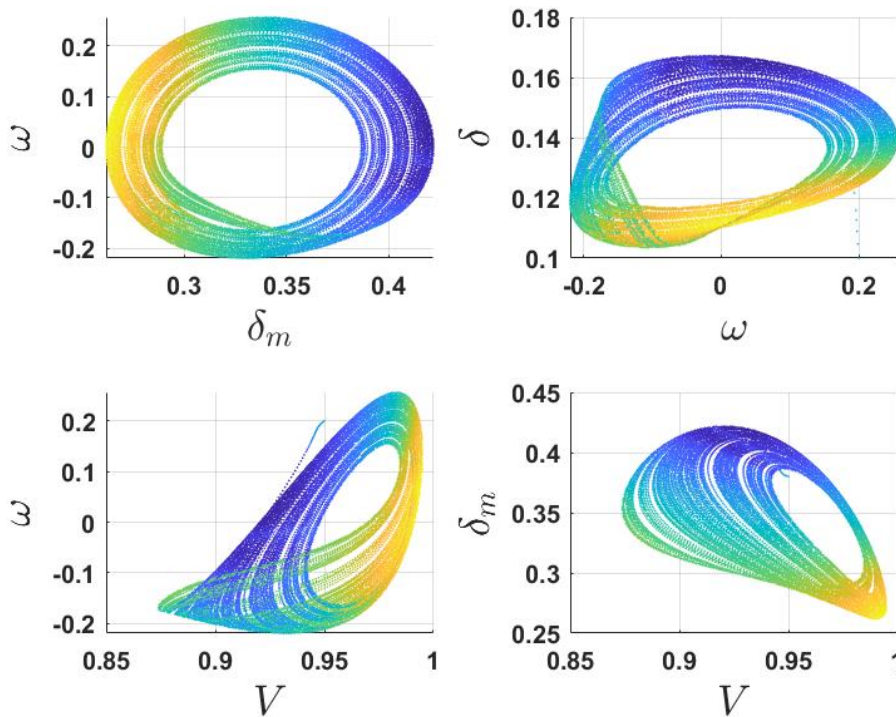


Figure 3. Several attractors from power system model Eq. (1).

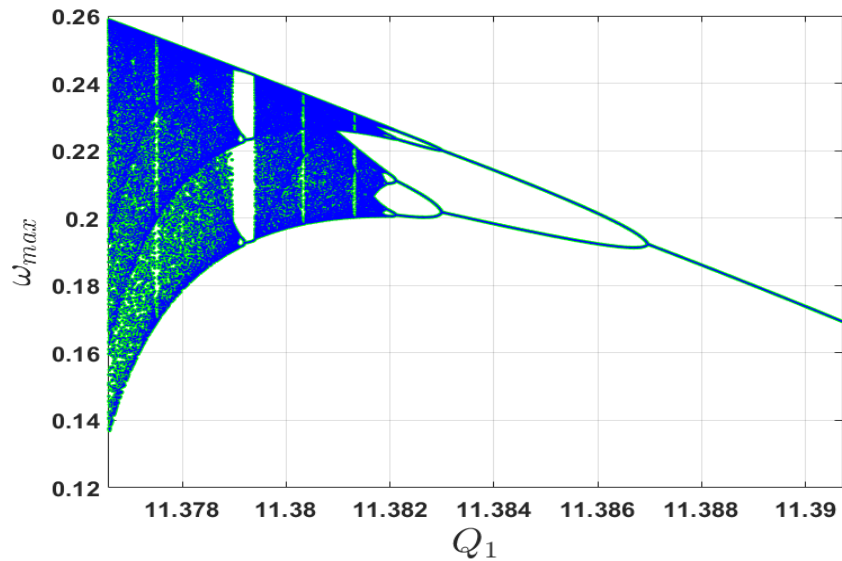


Figure 4. Bifurcation diagram of the considered system Eq. (1) showing local maxima in the ω state of the power system. Q_1 is the bifurcation parameter.

Another process of period-doubling bifurcation occurs in the range $Q_1 \in [11.382, 11.387]$; and in the interval, $Q_1 \in [11.3871, 11.3907]$, the power system behaves periodically. The Lyapunov exponent spectrum shown in Fig. 5 can show the aforementioned behaviors. Here, one of the calculated Lyapunov exponents is positive, as a result, the power system Eq. (1) has a chaotic nature. Fig. 6 shows the power spectral density and the bicoherence plot of the analyzed power system. The bicoherence is a measure used to present the nonlinear interactions between frequency components in a response of nonlinear systems. The chaotic behavior typically exhibits broadband frequency characteristics, which can be observed in the PSD and the bicoherence measures given in Fig. 6.

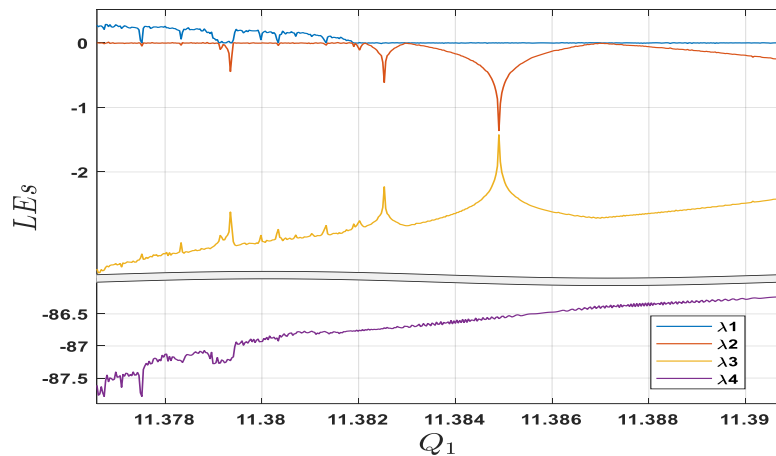


Figure 5. Lyapunov exponent spectrum for the power system Eq. (1) with Q_1 as bifurcation parameter.

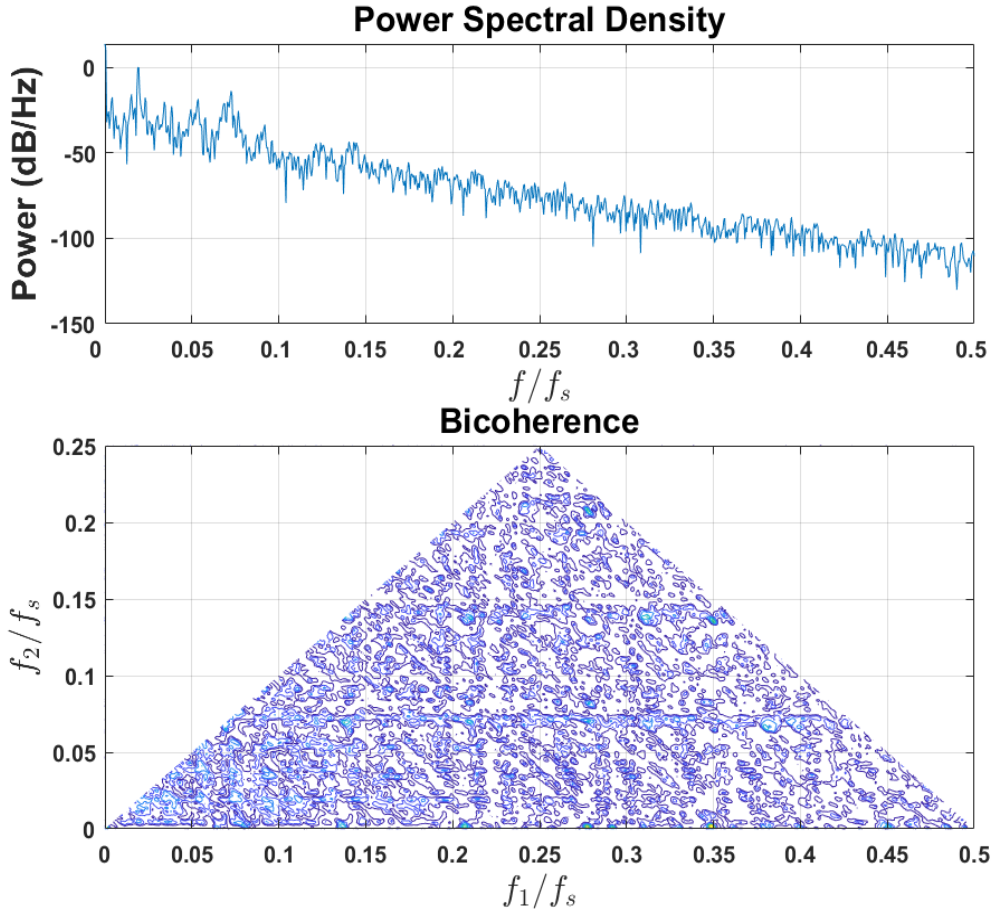


Figure 6. Power spectral density and bicoherence measurement for the power system Eq. (1).

The previous measures reveal that the chaos complex phenomenon exists in Eq. (1). The chaotic oscillation in power systems results in voltage instability and ends at voltage collapse and then can cause a severe blackout. Therefore, it is critical to construct a rigorous control mechanism to stabilize the power system's states and damp out unwanted chaotic oscillations, as will be done in the next section.

4. FIXED-TIME FRACTIONAL-ORDER SLIDING MODE CONTROLLER DESIGN

To implement the fixed-time sliding mode controller in a fractional-order sense, some mathematical preliminaries and definitions are necessary.

4.1. Preliminaries

Definition 1. The Caputo fractional-order derivative is defined as follows:

$${}_{t_0}^C D_t^\alpha f(t) = \begin{cases} \frac{1}{\Gamma(n-\alpha)} \int_{t_0}^t \frac{f^n(\tau)}{(t-\tau)^{\alpha+1-n}} d\tau, & n-1 < \alpha < n \\ \frac{d^n f(t)}{dt^n} & \alpha = n \end{cases}, \quad (2)$$

where α is refereeing to the fractional-order of the derivative; Γ refers to the gamma function.

Definition 2. The integral using Caputo definition in the fractional-order sense is as follows [23,24]:

$${}^c I_{t_0}^\alpha f(t) = {}^c D_{t_0}^{-\alpha} f(t) = \frac{1}{\Gamma(\alpha)} \int_{t_0}^t \frac{f(\tau)}{(t-\tau)^{1-\alpha}} d\tau \quad (3)$$

Property 1. For the derivative in Caputo sense, the following equality holds [23]:

$${}^c D_t^\alpha \left({}^c D_t^{-\beta} g(x(t)) \right) = {}^c D_t^{\alpha-\beta} g(x(t)) \quad (4)$$

where $\alpha \geq \beta \geq 0$.

Property 2. For the derivative in Caputo sense, the following equality is considered based on [25]:

$${}^c D_t^\alpha c = 0, \quad \text{where } c \text{ is any constant.} \quad (5)$$

Lemma 1. For the system defined below [26]:

$$\begin{cases} \dot{x} \leq -\eta \text{sig}(x)^p - \lambda \text{sig}(x)^q \\ x(0) = x_0 \end{cases}, \quad (6)$$

where parameters $\eta, \lambda, p, q > 0$ satisfying $p < 1, q > 1$ and $\text{sig}(\cdot)^\mu = |\cdot|^\mu \text{sign}(\cdot)$. Then the origin of system (6) is fixed time stable, and the settling time $T(x_0)$ will equal:

$$T(x_0) \leq T_{\max} \triangleq \frac{1}{\eta(1-p)} + \frac{1}{\lambda(q-1)} \quad (7)$$

4.2. Controller Design

The general system under control can be written as,

$$\dot{x} = f_i(x, t) + u_i \quad (8)$$

where x , and $f_i(x, t)$ are the state variable of the system and smooth nonlinear function, respectively. $i = 1, 2, \dots, N$, and u_i is the control signal for the nonlinear system. Define $e_i = x_i - x_{i_d}$ as the control error, where x_{i_d} represents the control objective. Then, the dynamical error will be as follows:

$$\dot{e}_i = \dot{x}_i - \dot{x}_{i_d} = f_i(x, t) + u_i - \dot{x}_{i_d} \quad (9)$$

To satisfy system (8) stability, define the sliding surface as follows:

$$s_i = D^{-\alpha}(\dot{e}_i + a_1 \text{sig}(e_i)^{p_1} + b_1 \text{sig}(e_i)^{q_1}) \quad (10)$$

where a_1, b_1 are positive parameters; $p_1 < 1, q_1 > 1$; $0 < \alpha < 1$. To drive the system (8) to reach the sliding surface (10) through the reaching phase within a fixed-time, then:

$$\dot{s}_i = D^{1-\alpha} D^\alpha(s_i) \quad (11)$$

$$= D^{1-\alpha}(\dot{e}_i + a_1 \text{sig}(e_i)^{p_1} + b_1 \text{sig}(e_i)^{q_1}) \quad (12)$$

$$= -a_2 \text{sig}(s_i)^{p_2} - b_2 \text{sig}(s_i)^{q_2} \quad (13)$$

where a_2, b_2 are positive parameters; $p_2 < 1, q_2 > 1$; then based on (13) and facts in Lemma 1, the sliding surface (10) will converge to zero within fixed-time, upper bounded by:

$$T_2 \leq \frac{1}{a_2(1-p_2)} + \frac{1}{b_2(q_2-1)} \quad (14)$$

At the end of the first phase of the sliding mode control known as the reaching phase, the sliding surface $s_i = 0$, then, its fractional derivative $D^\alpha s_i = 0$, therefore using (10) obtain,

$$\dot{e}_i = -a_1 \text{sig}(e_i)^{p_1} - b_1 \text{sig}(e_i)^{q_1} . \quad (15)$$

To prove the stability of Eq. (15), choose the Lyapunov function as follows:

$$V = |e_i| \quad (16)$$

Therefore, the time derivative of Eq. (16) will be:

$$\begin{cases} \dot{V} &= \text{sign}(e_i)\dot{e}_i \\ &= \text{sign}(e_i)(-a_1 \text{sig}(e_i)^{p_1} - b_1 \text{sig}(e_i)^{q_1}) \\ &= -a_1 \text{sign}(e_i)\text{sig}(e_i)^{p_1} - b_1 \text{sign}(e_i)\text{sig}(e_i)^{q_1} \end{cases} \quad (17)$$

Because of that $\text{sign}(e_i) \text{sig}(e_i) = 1$, then,

$$\begin{cases} \dot{V} &= -a_1 |e_i|^{p_1} - b_1 |e_i|^{q_1} \\ &= -a_1 V^{p_1} - b_1 V^{q_1} \end{cases} \quad (18)$$

Therefore, the dynamics begin the sliding phase motion, and based on (15), (18), and Lemma 1, the controlled system error e_i will converge to the dynamical system origin within a fixed-time ultimately limited by,

$$T_1 \leq \frac{1}{a_1(1-p_1)} + \frac{1}{b_1(q_1-1)} \quad (19)$$

Consequently, the dynamical system state x_i of the system (8) under the effect of the controller will reach the control required states x_{i_d} within fixed-time too. According to the sliding surface dynamic (13), the designed controller output can be determined enlightened by [27] as follows:

$$\begin{cases} u_i = -f_i(x, t) + \dot{x}_{i_d} - a_1 \text{sig}(e_i)^{p_1} - b_1 \text{sig}(e_i)^{q_1} \\ -D^{\alpha-1}(a_2 \text{sig}(s_i)^{p_2} + b_2 \text{sig}(s_i)^{q_2}) \end{cases} \quad (20)$$

The control signal (20), is an integral sliding mode controller based on fixed-time theory and fractional-order calculus, that can drive the controlled system (8) within a fixed-time to the origin. Due to the use of fractional calculus derivative and integral which have a filtering effect and the fact that $\text{sign}(x)|x|^\mu$ is continuous, the chattering will be avoided in the control signal.

4.3. Design of the Power System Chaotic Oscillation Controller

Eq. (1), will be used to derive the error dynamic model. When the error dynamic model reaches the origin through the designed controller, the power system leaves the chaotic state to the equilibrium state. The power system required states are $x_{2_d} = \omega_d = 0$ and $x_{4_d} = V_d = 1$, then errors can be written as $e_2 = \omega$ and $e_4 = V - 1$. Applying these transforms obtains:

$$\begin{cases} \dot{\delta}_m = f_1 \\ \dot{e}_2 = f_2 + u_2 \\ \dot{\delta} = f_3 \\ \dot{e}_4 = f_4 + u_4 \end{cases}, \quad (21)$$

where,

$$\begin{cases} u_2 = -f_2 + \dot{x}_{2d} - a_1 \text{sig}(e_2)^{p_1} - b_1 \text{sig}(e_2)^{q_1} \\ -D^{\alpha-1}(a_2 \text{sig}(s_2)^{p_2} + b_2 \text{sig}(s_2)^{q_2}) = P \\ u_4 = -f_4 + \dot{x}_{4d} - a_1 \text{sig}(e_4)^{p_1} - b_1 \text{sig}(e_4)^{q_1} \\ -D^{\alpha-1}(a_2 \text{sig}(s_4)^{p_2} + b_2 \text{sig}(s_4)^{q_2}) = Q \end{cases}$$

Using the designed fractional-order sliding mode control laws u_2 and u_4 , will drive the controlled system (21) to the required performance, and then the electrical power system will be stabilized within fixed-time.

5. SIMULATION RESULTS

To demonstrate the superiority, robustness, and the effectiveness of the proposed fixed-time fractional-order sliding mode controller, two illustrative scenarios have been presented for quenching the critical chaotic oscillation in the power system. The parameters in the control laws Eq. (20) are selected as follows: $a_1 = a_2 = 100$, $b_1 = b_2 = 100$, $p_1 = 0.9$, $q_1 = 1.2$, $p_2 = 0.67$, and $q_2 = 1.5$.

The controller is implemented in the first scenario at the start of the simulation, and the bifurcation parameter is selected such that $Q_1 = 11.377$, so the power system is chaotic. Fig. 7 shows the state variable's time-waveforms under the effect of the designed controller; obviously, the responses of the power system reach the control objectives with no chaotic oscillation and settle down toward equilibrium within finite time. Figs. 8 and 9, show the controlled system error variables e_2 and e_4 and the sliding surface function s_2 and s_4 , respectively. The system states approach the sliding surface as required under the proposed fixed-time fractional-order SMC controller. The implemented controller actions are given in Fig. 10. It is obvious that the controller outputs are smooth and chattering free as expected from the design. This renders the controller feasible for realistic applications. The physical significant of the u_2 control signal is a real power injected/absorbed using energy storage device (ESD). The energy storage device can be integrated to the generator bus or bus "1" in Fig. 1. On other hand the u_4 control signal represents reactive power Q injected/absorbed using any FACTS devices such as the SVC or STATCOM which allow the flexible and dynamic control of power systems. The FACTS device can be connected to the load bus or bus "2" in Fig. 1.

The second simulation case is prepared as follows: At first, the system works in chaos, and then at a certain moment "arbitrary one" the controller has been applied. The system state variables time waveforms are shown in Fig. 11, the controller has been activated at $t = 300(s)$. The state space trajectory is given in Fig. 12, it is obvious that the power system trajectory leaves the chaotic orbit just after applying the control signals and then follows the indicated red line in Fig. 12 toward the equilibrium within finite time.

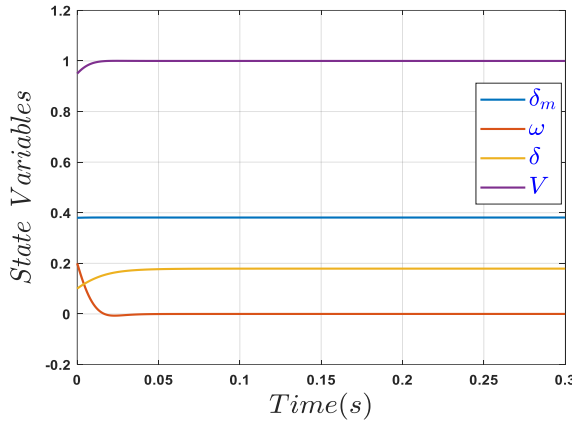


Figure 7. Time responses of the power system (1) where controller activated at $t = 0$ (s).

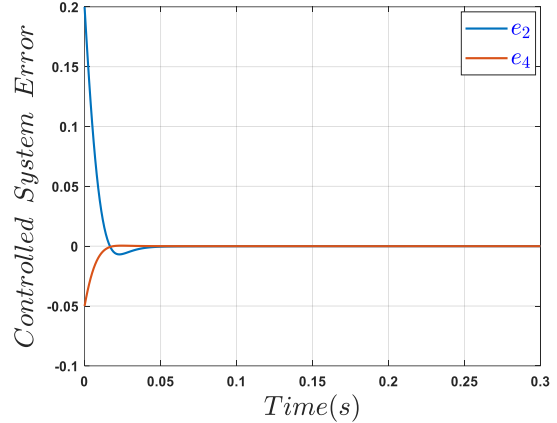


Figure 8. The controlled power system error time waveforms.

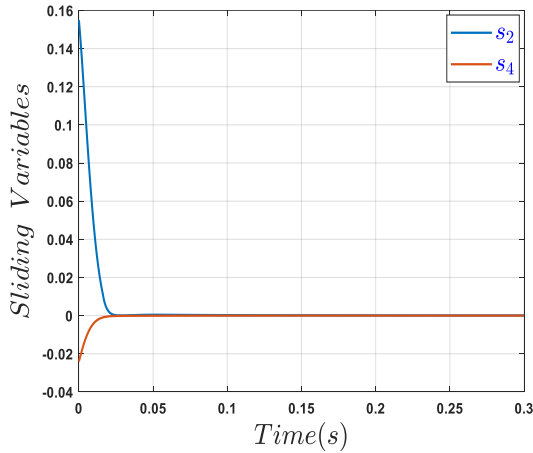


Figure 9. The sliding surfaces of the proposed controller.

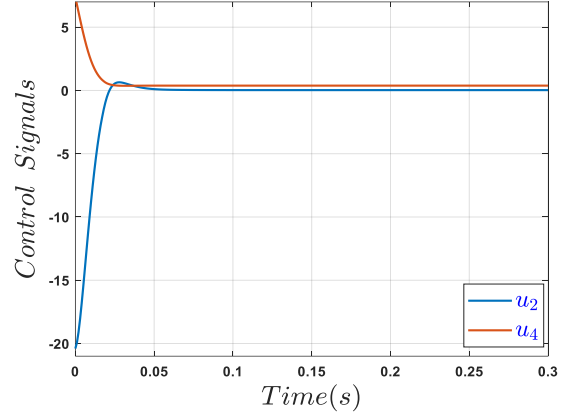


Figure 10. Controller outputs applied to the chaotic power system.

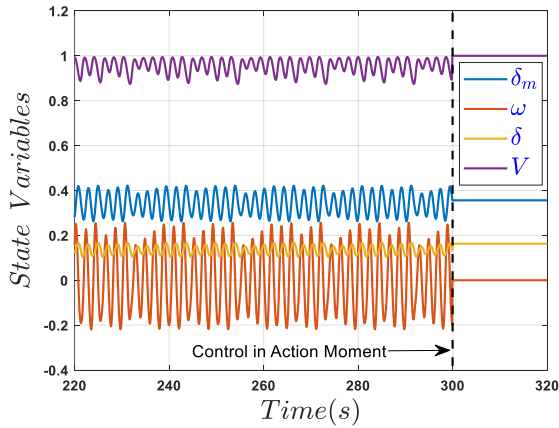


Figure 11. Time responses of the power system (1) where controller activated at $t = 300$ s.

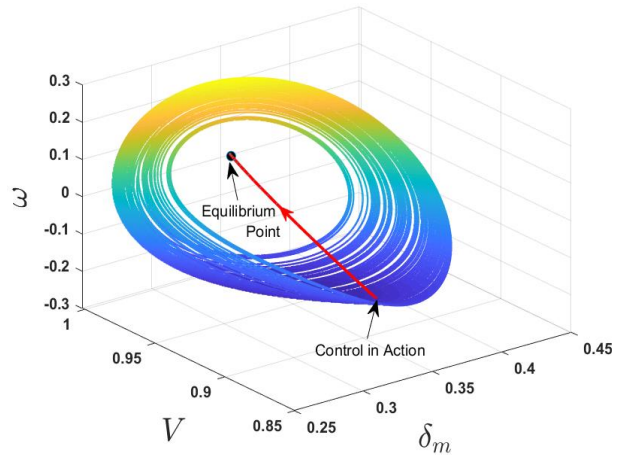


Figure 12. Orbit trajectory of the power system (1) where controller activated at $t = 300$ s. The red line part indicates the exit path from the chaotic attractor.

6. CONCLUSION

This paper presents an in-depth analysis of the phenomenon of chaotic oscillation in a power system. The nonlinear analysis tools, including bifurcation diagrams and Lyapunov exponent spectra, are employed to investigate this phenomenon. To mitigate the undesired chaotic oscillation in the electrical power system, a novel fixed-time fractional-order sliding mode controller is proposed. The controller effectively achieves the desired control objectives, exhibiting an ultimate response within a specified

upper-bound settling time. Notably, the control signals exhibit no chatter and facilitate a significant recovery of the chaotic power system towards synchronous operation. The stability of the controlled system is ensured through the application of Lyapunov stability theory during the controller design process. To validate the theoretical analysis, the superiority, effectiveness, and robustness of the control algorithm are evaluated across various application scenarios. The experimental results confirm the theoretical analysis, substantiating the exceptional performance of the proposed control algorithm.

REFERENCES

- [1] Zhao, H., Ma, Y.J., Liu, S.J., Gao, S.G. and Zhong, D. Controlling chaos in power system based on finite-time stability theory. *Chinese Physics B* 2011; 20(12): 120501. DOI: 10.1088/1674-1056/20/12/120501.
- [2] Gupta, P.C., Banerjee, A. and Singh, P.P. Analysis of global bifurcation and chaotic oscillation in distributed generation integrated novel renewable energy system. In: 2018 INDICON 15th IEEE India Council International Conference; 16-18 December 2018 :IEEE, pp. 1–5. DOI: 10.1109/INDICON45594.2018.8986983.
- [3] Dobson, I. and Chiang, H.D. Towards a theory of voltage collapse in electric power systems. *System Control Letter* 1989; 13(3): 253–262. DOI: 10.1016/0167-6911(89)90072-8.
- [4] Dobson, I., Chiang, H.D., Thorp, J.S. Fekih-Ahmed, L. A model of voltage collapse in electric power systems. In: 27th IEEE Conference on Decision and Control; 07-09 December 1988: IEEE, pp. 2104–2109. DOI: 10.1109/CDC.1988.194705.
- [5] Chiang, H.D., Dobson, I., Thomas, R.J., Thorp, J.S. and Fekih-Ahmed, L. On voltage collapse in electric power systems. *IEEE Transactions on Power systems* 1990; 5(2): 601–611. DOI: 10.1109/59.54571.
- [6] Chiang, H.D., Liu, C.W., Varaiya, P.P., Wu, F.F. and Lauby, M.G. Chaos in a simple power system. *IEEE Transactions on Power Systems* 1993; 8(4): 1407–1417. DOI: 10.1109/59.260940.
- [7] Kavasseri, R.G. and Padiyar, K.R. Analysis of bifurcations in a power system model with excitation limits. *International Journal of Bifurcation and Chaos* 2001; 11(09): 2509–2516. DOI: 10.1142/S0218127401003553.
- [8] Jing, Z., Xu, D., Chang, Y. and Chen, L. Bifurcations, chaos, and system collapse in a three node power system. *International Journal of Electrical Power & Energy Systems* 2003; 25(6): 443–461. DOI: 10.1016/S0142-0615(02)00130-8.
- [9] Wang, R.Q. and Huang, J.C. Effects of hard limits on bifurcation, chaos and stability. *Acta Mathematicae Applicatae Sinica* 2004; 20(3): 441–456. DOI: 10.1007/s10255-004-0183-x.
- [10] Harb, A.M. and Abdel-Jabbar, N. Controlling Hopf bifurcation and chaos in a small power system. *Chaos Solitons Fractals* 2003; 18(5): 1055–1063. DOI: 10.1016/S0960-0779(03)00073-0.
- [11] Wei, D.Q. and Luo, X.S. Passivity-based adaptive control of chaotic oscillations in power system. *Chaos Solitons Fractals* 2007; 31(3): 665–671. DOI: 10.1016/j.chaos.2005.10.097.
- [12] Al-Hussein, A.B.A., Tahir, F.R., Boubaker, O. Chaos elimination in power system using synergetic control theory. In: 2021 18th International Multi-Conference on Systems, Signals & Devices (SSD); 22-25 March 2021: IEEE, pp. 340–345. DOI: 10.1109/SSD52085.2021.9429398.
- [13] Al-Hussein, A.B.A., Tahir, F.R., Ouannas, A., Sun, T.C., Jahanshahi, H. and Aly, A.A. Chaos suppressing in a three-buses power system using an adaptive synergetic control method. *Electronics (Basel)* 2021; 10(13): 1532. DOI: 10.3390/electronics10131532.
- [14] Tang, X., Liu, Z. and Wang, X. Integral fractional pseudospectral methods for solving fractional optimal control problems. *Automatica* 2015; 62: 304–311. DOI: 10.1016/j.automatica.2015.09.007.
- [15] Wang, B., Xue, J., Wu, F. and Zhu, D. Stabilization conditions for fuzzy control of uncertain fractional order non-linear systems with random disturbances. *IET Control Theory & Applications* 2016; 10(6): 637–647. DOI: 10.1049/iet-cta.2015.0717.
- [16] Aghababa, M.P. Finite-time chaos control and synchronization of fractional-order nonautonomous chaotic (hyperchaotic) systems using fractional nonsingular terminal sliding mode technique. *Nonlinear Dynamics* 2012; 69(1): 247–261. DOI: 10.1007/s11071-011-0261-6.
- [17] Al-Hussein, A.B.A., Tahir, F.R. and Rajagopal, K. Chaotic power system stabilization based on novel incommensurate fractional-order linear augmentation controller. *Complexity* 2021; 2021. DOI: 10.1155/2021/3334609.
- [18] Polyakov, A. Nonlinear feedback design for fixed-time stabilization of linear control systems. *IEEE Trans Automat Contr* 2011; 57(8): 2106–2110. DOI: 10.1109/TAC.2011.2179869.

- [19] Al-Hussein, A.B.A., Tahir, F.R. and Pham, V.T. Fixed-time synergetic control for chaos suppression in endocrine glucose–insulin regulatory system. *Control Engineering Practice* 2021; 108: 1–11, DOI: 10.1016/j.conengprac.2020.104723.
- [20] Ma, C., Wang, F., Li, Z., Wang, J., Liu, C., Wu, W., Cheng, Y. Adaptive fixed-time fast terminal sliding mode control for chaotic oscillation in power system. *Math Probl Eng* 2018; 2018. DOI: 10.1155/2018/5819428.
- [21] Nayfeh, A.H., Harb, A.M. and Chin, C.M. Bifurcations in a power system model. *International Journal of Bifurcation and Chaos* 1996; 6(3): 497–512. DOI: 10.1142/S0218127496000217.
- [22] Das, P., Gupta, P.C. and Singh, P.P. Bifurcation, chaos and PID sliding mode control of 3-bus power system. In: *2020 3rd International Conference on Energy, Power and Environment: Towards Clean Energy Technologies; 05-07 March 2021*: IEEE, pp. 1–6. DOI: 10.1109/ICEPE50861.2021.9404493.
- [23] Aghababa, M.P. Design of a chatter-free terminal sliding mode controller for nonlinear fractional-order dynamical systems. *International Journal of Control* 2013; 86(10): 1744–1756. DOI: 10.1080/00207179.2013.796068
- [24] Rahman, Z.A.S., Jasim, B.H., Al-Yasir, Y.I., Hu, Y.F., Abd-Alhameed, R.A. and Alhasnawi, B.N. A new fractional-order chaotic system with its analysis, synchronization, and circuit realization for secure communication applications. *Mathematics* 2021; 9(20): 2593. DOI: 10.3390/MATH9202593.
- [25] Li, C. and Deng, W. Remarks on fractional derivatives. *Appl Math Comput* 2007; 187(2): 777–784. DOI: 10.1016/j.amc.2006.08.163.
- [26] Li, H. and Cai, Y. On SFTSM control with fixed-time convergence. *IET Control Theory & Applications* 2017; 11(6): 766–773. DOI: 10.1049/iet-cta.2016.1457.
- [27] Hung, S. and Wang, J. Fixed-time fractional-order sliding mode control for nonlinear power systems. *Journal of Vibration and Control* 2020; 26(17–18): 1425–1434. DOI: 10.1177/1077546319898311.